



Co addition for improved photocatalytic properties of ZnO nanoparticles

Ali Moulahi^{a,b*}



CrossMark

^a Chemistry Department, University College-Alwajh, Tabuk University, Tabuk, 71421 Saudi Arabia

^b Unit of Materials and Environment (UR15ES01), IPEIT, University of Tunis, 2 rue Jawaher Lel Nahru, Montfleury, 1089 Tunisia

Abstract

In this study, undoped ZnO and rod-like Co-doped ZnO nanoparticles (NPs) were successfully synthesized via one step polyol method. In this paper, $Zn(NO_3)_2 \cdot 6H_2O$ was used as a precursor and $Co(NO_3)_2 \cdot 6H_2O$ was the dopant. The morphology, structure, crystalline size and optical properties of the undoped and Co doped ZnO were measured in detail. The incorporation of the Co^{2+} in ZnO matrix was confirmed by DRX, ICP and EDX. Optical characterization of the sample revealed that the band gap energy (E_g) decreased from 3.36 to 3.25 eV with an increase in Co^{2+} doping concentration. The photocatalytic activity of the synthesized nanoparticles (NPs) was studied with respect to pure and Co-doped ZnO concentrations (0–10% Co). The improvement of photocatalytic activity has been noticed with the increase of Co concentration in ZnO nanoparticles.

Keywords: Polyol synthesis, ZnO NPs, Doping, Photocatalytic properties;

1. Introduction

Today, the recycling and remove of the toxic elements that exists in water is a big challenge on a global scale. Removal of these dye pollutants is necessary for both health and environmental considerations. Many strategies such as electrochemical oxidation, ozonation, photodegradation and adsorption had been used to remove the hazardous pollutants. Among these method, photodegradation process found particular interest because of its high efficiency and inexpensive. Methylene blue (MB) is one of the pollutants found in water from industrial waste. To remove the (MB) from the water, many types of adsorbents such as carbon materials [1], polymers [2] nanoparticles [3], nanocomposites [4] have been extensively used for the removal of dye from aqueous solution. In this study, we used the nanoparticles based ZnO and Co-doped ZnO to remove the MB. Basically, two factors, namely surface area and surface defects, are the most important variables to determine the photocatalytic properties of semiconductor. Due to its high surface activity, crystalline nature, morphological features, and texture; ZnO nanoparticles are considered as the most favorable catalyst for the degradation of organic pollutants [5]. ZnO is considered one of the most attractive materials, thanks to its higher optical

transmittance, wide direct band gap, large exciton binding energy of 60 meV, low cost and its low toxicity [6-8]. When it's a matter of getting attention, ZnO nanoscale is the best, due to its potential applications in many areas such as electronics, photonics and photocatalytic [9, 10]. ZnO crystallizes with a wurtzite structure and has a direct band gap of 3.36 eV at room temperature. A lot of studies prove that the physicochemical properties of the ZnO can be accomplished by doping [11, 12]. Actually, ZnO can be doped by many elements, such as Co [13], Fe [12], Cu [11], Ni [14], Mg [15] and Al [16], to meet the demands of different application. Among various dopants, Cobalt (Co^{2+}) ions is the promising candidate for the substitution of Zn sites. Co can be easily doped in the lattice of ZnO for its similar radius and electronic shell to Zn atom. Furthermore, it is possible to increase as well as decrease the band gap by the use of the right dopants, as opposed to size induced tuning, wherein the band gap can only be increased. In addition, recent literature reported that Cobalt nanoparticles exhibited excellent properties for degradation of the MB [4]. Doping of Co into ZnO is expected to modify the absorption, physical, and chemical properties of ZnO. By inducing more defects over the surface of ZnO, the optical adsorption

*Corresponding author e-mail: alimoulahi84@gmail.com; (Ali Moulahi).

Receive Date: 06 April 2021, Revise Date: 29 April 2021, Accept Date: 10 June 2021

DOI: 10.21608/ejchem.2021.71266.3564

©2021 National Information and Documentation Center (NIDOC)

properties can be enhanced. The synthesis of undoped and doped ZnO has been addressed by diverse methods like the vapor-phase transport [17], the microwave-assisted combustion method [18], the chemical vapor deposition [19], the magnetron sputtering [20], the laser ablation [21], and the wet chemical methods. The polyol process is now widely practiced and recognized among scientists in general and chemists in particular, it is a robust method in the wet chemistry field because of its operational simplicity, low cost, high efficiency, as well as the possibility of its environmentally safe large-scale production [22]. During this investigation, ZnO and Zn_{1-x}Co_xO were successfully elaborated via a polyol approach. The band gap values were adjusted by varying the doping concentration of Co. The influence of Co doping on the crystal structure, optical, morphological properties was studied. The effect of variation of Co doping concentration on the photocatalytic activity was studied.

2. Experimental section

2.1. Polyol synthesis

All of the chemical reagents were purchased from Aldrich and used without further purification steps. Zinc acetate dihydrate: Zn(CH₃COO)₂·2H₂O and cobalt nitrate hexahydrate: Co(NO₃)₂·6H₂O were used as zinc and cobalt sources and diethylene glycol (H₁₀C₄O₃) as template. In a common synthesis, zinc and cobalt precursors are brought in a stoichiometric proportion in order to get 1 g of Zn_{1-x}Co_xO powder and added to 250 mL H₁₀C₄O₃. The resulting mixture was heated under continuous stirring to obtain a green sol refluxed at 180 °C for 1 h. At the end of the reaction, the precipitate was separated by centrifugation, washed several times with ethanol to remove the organic product and dried in an oven at 80 °C.

2.2. Characterization techniques

X-ray powder diffraction data (XRD) were recorded on a X'PertPro Panalytical diffractometer with CuK α radiation ($\lambda=1.5418$ Å) and a graphite monochromator. The XRD measurements were carried out by applying a step scanning method (2 θ range from 3 to 80°), the scanning rate is 0.017 per second and the step time is 1 s. Scanning electron microscopy (SEM) images were carried out with a SEI instrument (operating at 5 kV) microscope. The diffuse reflectance of our pigment particles were measured using a Varian Cary 5000 UV-Vis-NIR spectrophotometer in 250 nm–800 nm range.

2.3. Measurement of Photocatalytic Activity

The photocatalytic activity of the undoped ZnO and Co-doped ZnO was tested by the methylene blue (MB) dye degradation under UV-Vis irradiation.

Experiments were performed in a Vossloh schwabe (1 L) reactor containing 10 mL of MB solution with an initial concentration of 10 mg L⁻¹ and the loading of the catalyst is 1 g L⁻¹. The irradiation source was under the irradiation of UV lamp (125 W) with a maximum emission at 365 nm immersed within the reactor in a double wall jacket for water circulation to avoid the heating of mixture. The MB dye solution was mixed with a fixed amount ZnO NPs at natural pH=7.4. The solution was placed under UV illumination and was magnetically stirred.

At regular time intervals, suspension samples were collected and centrifuged to separate solid particles. The filtrates were analyzed by recording the variation of the absorption band maximum at 365 nm in the UV–vis spectrum of MB using a Hach RD/4000 UV–vis spectrophotometer. Similar procedure was adopted for Co dopants (1, 5, and 10%)-ZnO using MB solution. The MB concentration was calculated by Beer–Lambert equation.

Percentage of MB degraded by the catalyst surface was calculated from the following equation:

$$\text{Percentage of degradation} = (C_0 - C_t) / C_0 \times 100\%$$

where C₀ represents the initial time of absorption and C_t represents the absorption after various intervals of time (0, 30, and 60 min).

3. Results and discussion

3.1. Structure and morphology

The structure and the crystallinity of the pure ZnO and Co-doped ZnO were performed using X-ray diffraction (XRD) (Figure 1). For the undoped samples (Figure 1a), the XRD analysis reveals the presence of narrow peaks, suggesting the high crystallinity of the material and the all peaks perfectly indexed to ZnO wurtzite structure (JCPDS: 36-1451). For the Co doped ZnO all the peaks of the samples match well with the standard diffraction data for a hexagonal zincite structure of ZnO. No diffraction peaks of impurities such as CoO emerges for Co-doped ZnO, and no peaks associated with other crystalline forms were detected, which most likely indicates that doping Co atoms substituted Zn atoms at lattice. It is noted that the all peaks are indexed to ZnO hexagonal phase but we noted that the intensity of the XRD peak decreases with increase in Co doping concentration along with an increase in its full width at half maxima (FWHM) (shown in Figure 1a–d) which confirms the slender loss in their crystallinity due to distortion of lattice. This indicates that most of the Co²⁺ ions go into the lattice as substitution ions to

replace the Co^{2+} ions and do not enter the void spaces. Since the ionic radius of the substituted Co^{2+} ($R_{\text{Co}^{2+}} = 0.058 \text{ nm}$ is 0.58 \AA) is smaller than Zn^{2+} ($R_{\text{Zn}^{2+}} = 0.06 \text{ nm}$ is 0.60 \AA). Furthermore, the cell Parameters of hierarchical Co doped ZnO nanorods are obtained from Rietveld analysis. The decrease of c-axis is also given reasonable explanation. The calculated lattice parameters are listed in Table 1. It is observed from Table 1 that there is an alteration in its lattice parameter values as Co^{2+} ion substitutes Zn^{2+} ion in the lattice. As the doping concentration increases, the dopant atom incorporated occupies the substitutional lattice site.

When we enlarged (zoom) the XRD part between 30° and 36° we show a small shift of diffraction peaks to higher angles which confirmed the incorporation of the Co^{2+} in ZnO matrix.

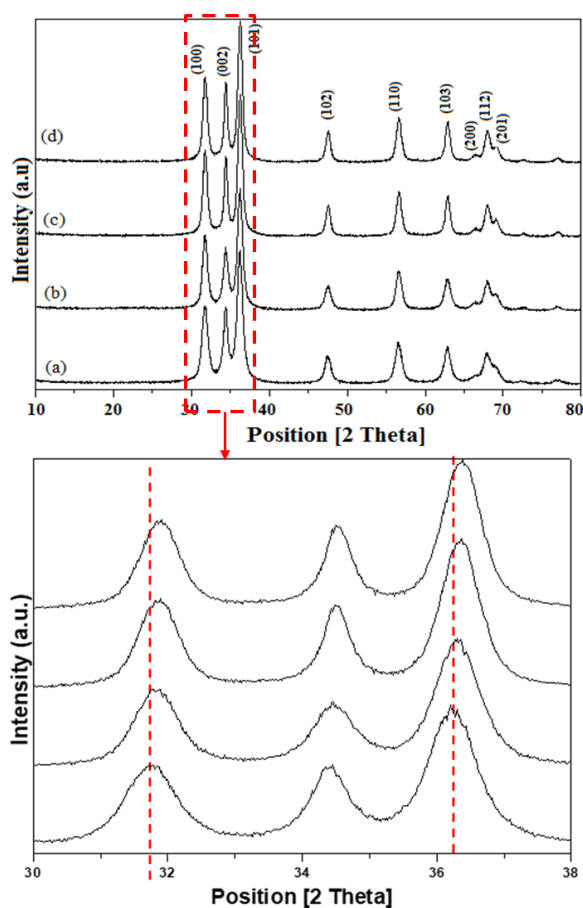


Fig. 1. X-ray diffraction patterns for various Co-doped ZnO oxides obtained by polyol process. a) ZnO, b) 1% Co doped ZnO, c) 5% Co doped ZnO and d) 10% Co doped ZnO.

The crystalline sizes of the samples (a)-(d) can be estimated from the full width at half-maximum diffraction peak by using Scherrer equation.

$$L = 0.89\lambda / \beta \cos\theta$$

Where L is the average crystallite size in nm, $\lambda = 0.154056 \text{ nm}$, β is the full width at the half maximum, and θ is the diffraction angle. The average crystallite size values, calculated from XRD patterns of the samples synthesized with the molar ratio 0% Co, 1% Co, 5% Co and 10% Co, have been found to be, about 98, 85, 77 and 60 nm, respectively.

The evolution of the efficient Co^{2+} concentration versus the target one is plotted in Figure 2. The dependency of the efficient concentration versus the target concentration is clearly linear and the curve's slope indicates that half the Co^{2+} ions in the raw polyol medium are efficiently introduced in the $\text{Zn}_{1-x}\text{Co}_x\text{O}$ compounds.

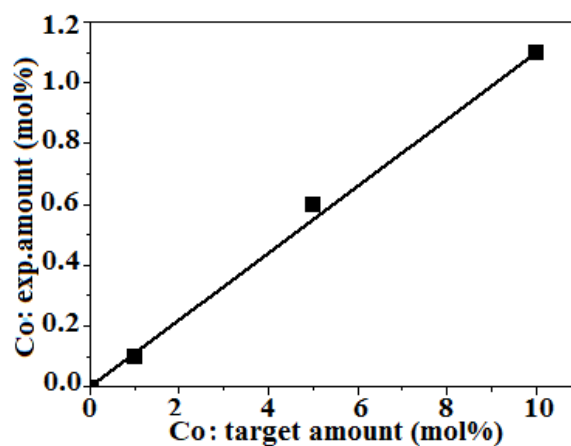


Fig. 2. Co^{2+} concentration efficiently introduced in Co-doped ZnO particles versus the Co^{2+} target concentration.

The morphologies and microstructures of pure ZnO and Co-doped ZnO nanostructures were investigated by SEM. Figure 3 show the SEM images of pure ZnO (Figure 3a and b) and $\text{Zn}_{1-x}\text{Co}_x\text{O}$ (Figure 3c-f). It is clear that the morphology of the pure ZnO is quite different from those obtained in presence of the Co. Comparative experiments have shown that pure ZnO consists of spheres like nanostructures. With 1% Co doped, irregular nanoparticles of rods and spheres were generated (Fig. 3c and d). With increasing of the Co concentration from 1% to 5% and 10% (Figure 3e-h), the materials consist of a homogenous phase of uniform nanorods. After SEM analysis we can conclude that the amount Co has clear effects on the formation of nanorods.

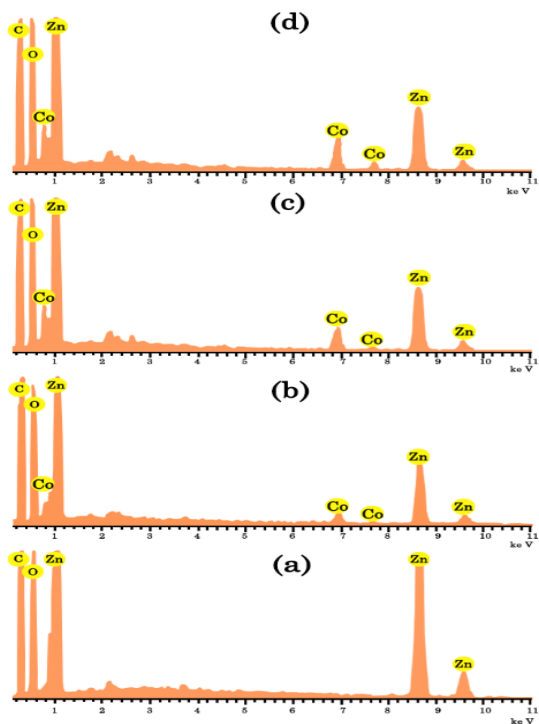


Fig. 3. SEM images of ZnO (a, b), 1% Co doped ZnO (c, d), 5% Co doped ZnO (e, f) and 10% Co doped ZnO (g, h).

The characterization of the chemical composition of the as-synthesized undoped and Co doped ZnO was studied by Energy Dispersive X rays spectroscopy (EDX). The EDX spectrum shown in Fig. 4 proves that the as-synthesized 1%, 5% and 10% Co-doped ZnO consists of oxygen, zinc and Cobalt which is in agreement with the results of X-ray diffraction and ICP. The weak signals relating to the carbon atoms come from the electron microscope grid.

3.2. Optical properties

The optical properties of the pure ZnO NPs and Co-doped ZnO nanostructure was studied by UV-Vis absorption. The UV-vis absorption spectra of the samples are presented in (Figure 5).

It is found that the absorption peak increases with the doping concentration. The increase in absorbance may be due to miscellaneous factors like particle size, oxygen deficiency, and defects in grain structure. All samples showed similar UV-vis absorption spectra which demonstrate a broad intense absorption from about 370 nm. It is observed also that the absorption edge of Co-doped ZnO NPs is shifted to the longer wavelength, this shift may be explicated the small amount of lattice strain present in the sample as a result of Co dopant towards ZnO. As a matter of fact, ZnO is a direct band gap semiconductor, and therefore its

absorption coefficient is associated to the excitation energy by $\alpha h\nu = (h\nu - E_g)^n$ where n is an exponent, n is the frequency of the incident radiation, h is the Plank's constant, and E_g is the optical energy gap of the material.

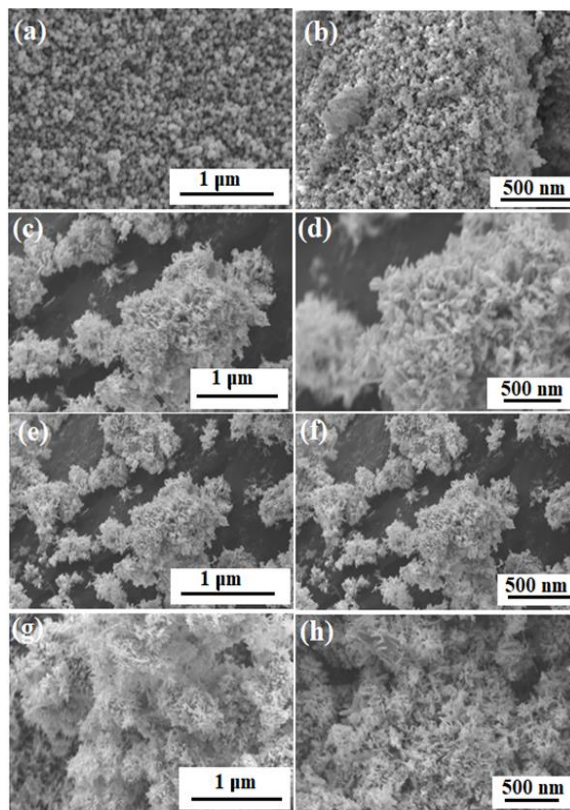


Fig. 4. EDX of ZnO (a), 1% Co doped ZnO (b), 5% Co doped ZnO (c) and 10% Co doped ZnO (d).

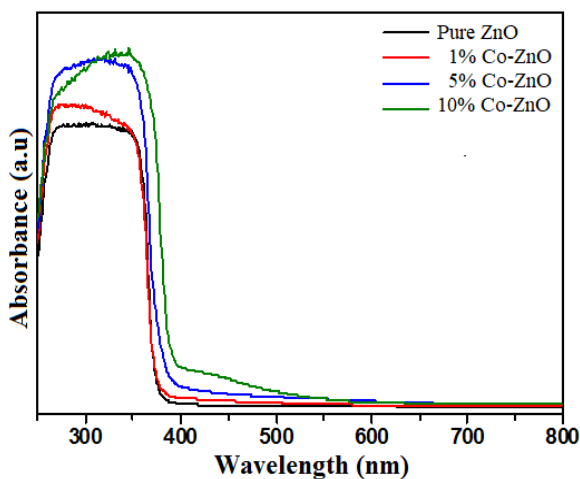


Fig. 5. Optical absorption of undoped ZnO and Co-doped ZnO.

To obtain the absorption onset $(\alpha h\nu)^2$ was plotted vs. energy $h\nu$ (Figure 6). The absorption onsets obtained in Figure 6 indicate that they all at the range

of 3.36–3.25 eV. Extrapolation of the linear part until its intersection with the $h\nu$ axis gives the values of E_g . From Figure 5, E_g values are 3.36, 3.32, 3.29 and 3.25 eV for pure ZnO, 1%Co-doped ZnO, 5%Co-doped ZnO and 10%Co-doped ZnO respectively. Both of them showing a red shift compared to the undoped ZnO (3.36 eV) which may be due to the size effect. The red shift and decrease in band gap energy (E_g) confirm the presence of Co^{2+} inside the Zn^{2+} site of the ZnO lattice.

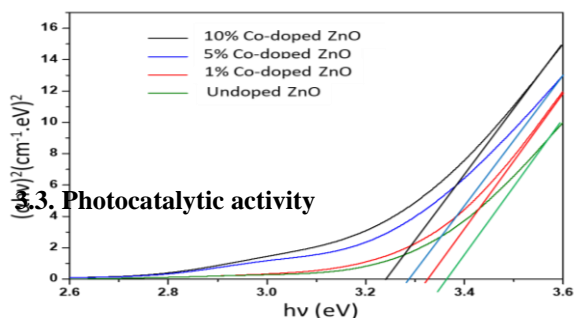


Fig. 6. Band gap energy (E_g) for pure and Co-doped ZnO NPs.

The photocatalytic degradation study of pure ZnO and Co-doped ZnO with photodegradation of methylene blue (MB) was studied under different intervals of time (0–60 min). The optical absorption spectra of MB solution at different time intervals (0–60 min) were recorded and the same is illustrated by Figure 7. It is observed that with the lapse of time the peak height decreases indicating greater degradation of MB due to the photocatalytic activity of ZnO. A negligible amount of the MB has been degraded using pure ZnO after 60 min, whereas the 10% Co-doped ZnO sample revealed higher degradation efficiency. Indeed, the concentration of MB decreased as the visible light exposure time was increased. We detected that the 10%Co-ZnO nanorods yielded more photodegradation compared to that of pure ZnO.

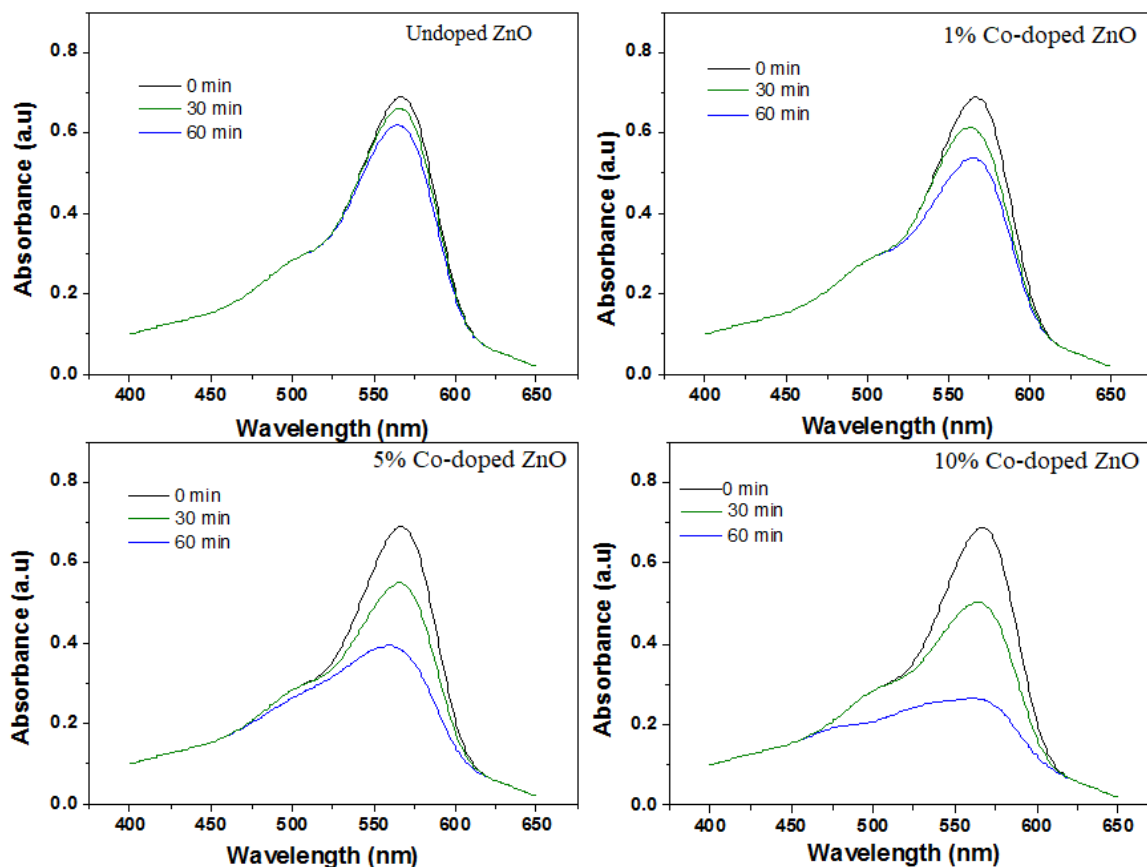


Fig. 7. Absorption spectra decrement of methylene blue (MB) aqueous solution degraded from (0–60 min)

Figure 8 shows the percentage of degradation for pure and Co-doped ZnO nanorods. It is observed that 10% Co-doped ZnO has exhibited a maximum degradation of 93% compared with the other doping concentrations (Table 2). Such values nicely compared with values reported in the literature Table 3. Recently, Giahi et al. [23] prepared Mg doped TiO₂ nanoparticles via the sol-gel method and tested for degradation of rhodamine B, nonylphenol ethoxylates, pseudoephedrine hydrochloride, and nicotine. The photocatalytic degradation shows that 98.92, 98.00, 98.00 and 97.95% of rhodamine B, nonylphenol ethoxylates, pseudoephedrine hydrochloride, and nicotine was decomposed by Mg-doped TiO₂, respectively. Ethiraj et al. [24] studied for the first time the photodegradation of phenol by the Cu-NiO. The nanocatalyst efficiency for phenol removal was tested in real leather industrial wastewater effluent which could remove about 85.7% within 150 min.

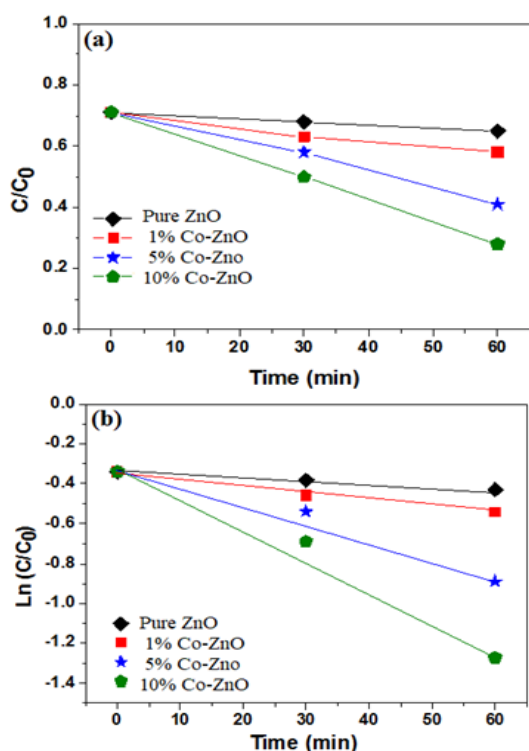


Fig. 8. Photodegradation of MB under pure and Co doped ZnO

The enhanced photocatalytic activity observed from Co-doped ZnO due to presence of defects and oxygen vacancies created by Co doping inside the ZnO matrix. The reaction kinetics can be observed by plotting linear curves for the concentration ratio, $\ln(C/C_0)$, against the irradiation time “t”. From the curve (Figure 9a), it is obviously clear that the existence of Co ions from 1 to 10% inside the ZnO matrix has actually activated the photocatalytic process. It was reported that the photocatalytic activity count basically on

optical properties, particle size and morphology of the material [15]. When the data are plotted as logarithms of normalized dye concentration versus time, linear plots are obtained (Fig.9b). Their equation is as follows:

$$\ln(C/C_0) = kt$$

Which C is the concentration at the instant t, C_0 is the initial concentration and k is the kinetic constant. This indicates that the decomposition follows first-order kinetics; the values k, which are actually the slopes of the lines obtained, are calculated and it was 1.11×10^{-3} , 3.01×10^{-3} , 0.47×10^{-2} , and 1.55×10^{-2} for the pure ZnO nanospheres, 1% Co-ZnO nanoparticles, 5% Co-ZnO nanoparticles, and 10% Co-ZnO nanorods respectively. Among them, the 5% Co-ZnO and 10% Co-ZnO nanoparticles have exhibited the highest degradation rate constant (k) value, which has quite remarkably raised compared with that of pure ZnO NPs.

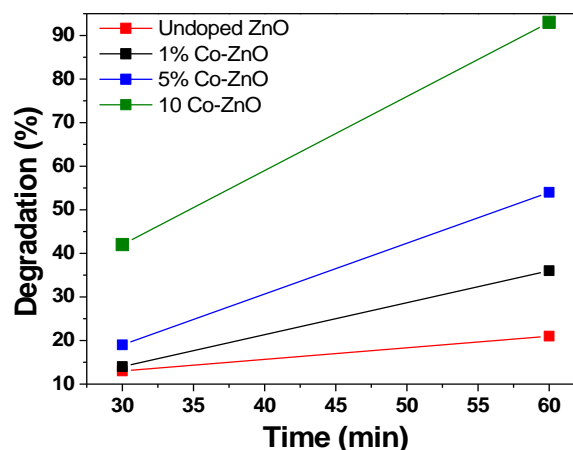


Fig. 9. Photocatalytic degradation of MB on the undoped ZnO and Co doped ZnO NPs under UV light irradiation (a) and first order linear transforms of disappearance of MB (b).

4. Conclusion

To conclude, the polyol technique is a successful route of pure ZnO NPs and Co-doped ZnO synthesis. Effect of “Co” doping on structural, morphological, optical and photocatalytic activity of ZnO nanoparticles is tested. The XRD and SEM validated that the crystallite size decreased with increase in Co content. For the highest dopant concentration, the morphology is totally modified with the formation of nanorods. In comparison with pure ZnO, Co-doped ZnO rod-like displayed a strengthened photocatalytic performance under mild UV-light irradiation in the methylene blue photodegradation experiments at ambient temperature, which may be connected to

specific site-selective photocatalytic behavior related to Zn sites.

5. Conflicts of interest

The authors declare no conflict of interest.

6. Notes

The author declare no competing financial interest.

7. References

- [1] B. Maazinejad, O. Mohammadni, G. A.M. Ali, A. S.H. Makhlof, M. N. Nadagouda, M. Sillanpää, A. M. Asiri, S. Agarwal, V. K. Gupta, H. Sadegh. Taguchi L9(34) orthogonal array study based on methylene blue removal by single-walled carbon nanotubes-amine: Adsorption optimization using the experimental design method, kinetics, equilibrium and thermodynamics, *J. Molecular Liquids* 298 (2020) 112001.
- [2] S. Agarwal, H. Sadegh, M. Monajjemi, A. S. Hamdy, G. A.M. Ali, A. O.H. Memar, R. Shahryari-ghoshekandi, I. Tyagi, V. K. Gupta. Efficient removal of toxic bromothymol blue and methylene blue from wastewater by polyvinyl alcohol. *J. Molecular Liquids* 218 (2016) 191-197.
- [3] K.A. Isai, V.S. Shrivastava, Photocatalytic degradation of methylene blue using ZnO and 2%Fe-ZnO semiconductor nanomaterials synthesized by sol-gel method: a comparative study, *SN Applied Sciences* (2019) 1:1247 | <https://doi.org/10.1007/s42452-019-1279-5>.
- [4] H. H. A. Ghafar, G. A.M. Ali, O. A. Fouad, S. A. Makhlof. Enhancement of adsorption efficiency of methylene blue on Co₃O₄/SiO₂ nanocomposite, *J. Desalination and Water Treatment* 53/11 (2015) 2980-2989.
- [5] J. Lv, W. Gong, K. Huang, J. Zhu, F. Meng, X. Song, Z. Sun, Effect of annealing temperature on photocatalytic activity of ZnO thin films prepared by sol-gel method, *Superlattices Microstruct.* 50 (2011) 98-106.
- [6] E.F.M. El-Zaidia, A.A.A. Darwish, Electronic properties and photovoltaic performance of VONc-ZnO hybrid junction solar cells, *Synthetic Metals* 259 (2020) 116227.
- [7] S. P. Singha, S. K. Sharma, D.Y. Kim, Carrier mechanism of ZnO nanoparticles-embedded PMMA nanocomposite organic bistable memory device, *Solid State Sci.* 99 (2020) 106046.
- [8] S. Pearton, D. Norton, K. Ip, Y. Heo, T. Steiner, Recent advances in processing of ZnO, *J. Vac. Sci. Technol. B: Microelectron. Nanometer Struct. Process. Meas. Phenom.* 22 (2004) 932-948.
- [9] J. Wang, R. Chen, X. Lan, K. Sridhar, Synthesis, Properties and applications of ZnO nanomaterials with oxygen vacancies: a review, *Ceram. Int.* 44(2018) 7357-7377.
- [10] A. Moulahi, F. Sediri, Pencil-like zinc oxide micro/nano-scale structures: Hydrothermal synthesis, optical and photocatalytic properties, *Mater. Res. Bull.*, 48 (2013)3723-3728.
- [11] L.C.-K. Liao, J.-S. Huang, Energy-level variations of Cu-doped ZnO fabricated through sol-gel processing, *J. Alloys Compd.* 702 (2017) 153-160.
- [12] A. Hui, J. Ma, J. Liu, Y. Bao, J. Zhang, Morphological evolution of Fe doped seaurchin-shaped ZnO nanoparticles with enhanced photocatalytic activity, *J. Alloys Compd.* 696 (2017) 639-647.
- [13] I. Mjejri, S. Mornet, M. Gaudon, From nano-structured polycrystalline spheres with Zn_{1-x}CoxO composition to core-shell Zn_{1-x}CoxO@SiO₂ as green pigments, *J. Alloys Compd.* 777 (2019) 1204-1210.
- [14] K. Xu, C. Liu, R. Chen, X. Fang, X. Wu, J. Liu, Structural and room temperature ferromagnetic properties of Ni doped ZnO nanoparticles via low-temperature hydrothermal method, *Phys. B Condens. Matter* 502 (2016) 155-159.
- [15] R. E. Adam, H. Alnoor, G. Pozina, X. Liu, M. Willander, O. Nur, Synthesis of Mg-doped ZnO NPs via a chemical low-temperature method and investigation of the efficient photocatalytic activity for the degradation of dyes under solar light. *Solid State Sci.* 99 (2020) 106053.
- [16] X. Xing, D. Deng, Y. Li, N. Chen, X. Liu, Y. Wang, Macro-/nanoporous Al-doped ZnO via self-sustained decomposition of metal-organic complexes for application in degradation of Congo red, *Ceram. Int.* 42 (2016) 18914-18924.
- [17] G.S. Kim, S.J. Kim, R. Mohan, ZnO nanostructures in vapor transport growth method, *Sci. Adv. Mater* 6 (2014) 1-7.
- [18] Pengli Zhu, Jingwei Zhang, Zhishen Wu, and Zhijun Zhang, Microwave-Assisted Synthesis of Various ZnO Hierarchical Nanostructures: Effects of Heating Parameters of Microwave Oven, *Cryst. Growth Des.*, 8 (2008) 3148-3153.
- [19] J. Zhang, L. Sun, J. Yin, H. Su, C. Liao, C. Yan, Control of ZnO Morphology via a Simple Solution Route *Chem. Mater.* 2002, 14, 4172.

-
- [20] H.Q. Dai, H. Xu, Y.-N. Zhou, F. Lu, Z.-W. Fu, J. Physical Chem. C, 116 (2012) 1519-1525.
- [21] H. Usui, Y. Shimizu, T. Sasaki, N. Koshizak, J. Phys. Chem. B 109 (2005) 120-124.
- [22] I. Trenque, S. Mornet, E. Duguet, M. Gaudon, New Insights into Crystallite Size and Cell Parameters Correlation for ZnO Nanoparticles Obtained from Polyol-Mediated Synthesis, Inorg. Chem. 52 (2013) 12811-12817.
- [23] M. Giahi, D. Pathania, S. Agarwal, G. A. M. Ali, K. F. Chong, V. K. Gupta, preparation of Mg-doped TiO₂ nanoparticles for photocatalytic degradation of some organic pollutants. Studia UBB Chemia 64(1) (2019) 7-18. DOI:10.24193/subbchem.2019.1.01
- [24] A.S. Ethiraj, P. Uttam, Varunkumar K, K. F. Chong, G. A.M.Ali, Photocatalytic performance of a novel semiconductor nanocatalyst: Copper doped nickel oxide for phenol degradation. Materials Chemistry and Physics, 242 (2020) 122520.